16th Triennial World Congress, Prague, Czech Republic

NONLINEAR BACKSTEPPING DESIGN OF ANTI-LOCK BRAKING SYSTEMS WITH ASSISTANCE OF ACTIVE SUSPENSIONS

Wei-En Ting and **Jung-Shan Lin** [1]

Department of Electrical Engineering
National Chi Nan University
301 University Road, Puli
Nantou, Taiwan 545, R.O.C.

Abstract: This paper develops a nonlinear anti-lock braking system combined with active suspensions applied to a quarter-vehicle model by employing nonlinear backstepping control design schemes. An anti-lock braking system must have the potentials to release the wheel-locking situation and assist the car to stop at shorter distance. Although the braking distance can be reduced by the control torque from disk/drum brakes, the braking time and distance could be further improved if the normal force generated from active suspension systems is considered simultaneously. As a result, the integration of anti-lock braking and active suspension systems indeed possesses the ability to enhance the system performance because of reduction of braking time and distance. Furthermore, some comparative simulations are given to illustrate the excellent performance of our integrated anti-lock braking system. *Copyright © 2005 IFAC*

Keywords: Antilock braking systems, Active vehicle suspension, Nonlinear control

1. INTRODUCTION

With advanced development of vehicular technology, the safety requirement for automobiles becomes more and more important. The techniques applied for various vehicles have already improved system stability and passenger safety with the use of several significant control systems, such as anti-lock braking systems (Alvarez *et al.*, 2003; Drakunov *et al.*, 1995; Liu and Sun, 1995; Unsal and Kachroo, 1999), active suspension systems (Kim, 1996; Lin and Kanellakopoulos, 1997), traction control systems (Drakunov *et al.*, 2000) and so forth, popularly used in automobile industries. Recently, there are some integrated studies which combine the previous mentioned subsystems in order to further enhance vehicle dynamics to reach better efficiency. For example, the concept of integrating anti-lock braking systems with active suspensions has been introduced and investigated in (Alleyne, 1997).

Many theories and design methods for anti-lock braking systems (ABS) and active suspension systems have been proposed individually by several literatures for decades. ABS is the mechanism to manipulate the braking of automobiles to prevent from uncontrollable skidding in accidents due to locking of wheels. It can provide the directional stability and shorten the braking distance. Various researchers have considered a slip-ratio control of anti-lock braking systems in the use of sliding mode control schemes (Drakunov *et al.*, 1995; Unsal and Kachroo, 1999). In (Liu and Sun, 1995),

[1] This work was supported in part by National Science Control, Taiwan, R.O.C., under the Grant NSC 92-2213-E-260-013. (Email: jslin@ncnu.edu.tw)

a gain-scheduling scheme was proposed for the optimal target slip tracking of an anti-lock braking system, where the friction coefficient varies with respect to different vehicle forward speeds.

Active suspension systems must have the potentials to guarantee ride comfort of passengers. Hence, in the design of active suspensions, the improvement of ride quality is the major control objective to be emphasized. In (Lin and Kanellakopoulos, 1997), a novel nonlinear backstepping design (Khalil, 2002; Krstić *et al.*, 1995) has been developed for a quarter-car active suspension system which aims to improve the tradeoff between the ride quality of passenger comfort and the utilization of suspension travel. In addition, a nonlinear indirect adaptive controller has been applied to the design of a quarter-car active suspension with a hydraulic actuator in (Kim, 1996).

The target of this paper is to take advantage of anti-lock braking systems combined with active suspensions to further reduce the vehicle braking time and distance. During braking process, if the vertical normal force is increased (this situation is equivalent to the increase of the weight of a car), the friction force between the car and road surface is increased to help the vehicle to stop at a shorter distance. However, the normal force can not be increased naturally, so active suspensions should be the tools employed to achieve the adjustment of normal force. With the choice of an appropriate integrated algorithm, the vertical normal force can be adjusted with the braking torque in order to achieve the reduction of braking time and distance.

The remainders of this paper are organized as follows. In Section 2, the system dynamics of a quarter-vehicle model is introduced, including both anti-lock braking and active suspension systems. In Section 3, nonlinear backstepping control schemes are employed for the design of this quarter-car integrated braking system. The simulation results are illustrated in Section 4, and some concluding remarks are given in Section 5.

2. SYSTEM MODEL AND DYNAMICS

In general, the quarter-vehicle braking model can be shown in Fig. 1. According to Newton's second law, the dynamics of the quarter-car braking system can be represented by the following equations:

$$\begin{aligned} m\dot{v} &= -F_z\mu(\lambda) - C_x v^2 \\ I\dot{\omega} &= -B\omega + F_z\mu(\lambda)R - \tau_b \\ \dot{\tau}_b &= -\frac{1}{\tau}\tau_b + \frac{K_b}{\tau}v_b\,, \end{aligned} \tag{1}$$

where m is the total mass consisting of the car body and wheel, v is the longitudinal velocity, ω is the angular velocity, τ_b is the braking torque applied by the disk/drum brakes, I is the wheel's moment of inertia, B is the friction coefficient due to the wheel bearings, F_z is the vertical normal force on the road, R is the radius of the wheel, C_x is the aerodynamic coefficient of the vehicle, and $\mu(\lambda)$ is the friction coefficient between tire and road to be defined later. In addition, the braking torque is controlled by the braking pressure v_b from the braking pedal, where τ is the time constant and K_b is the braking gain.

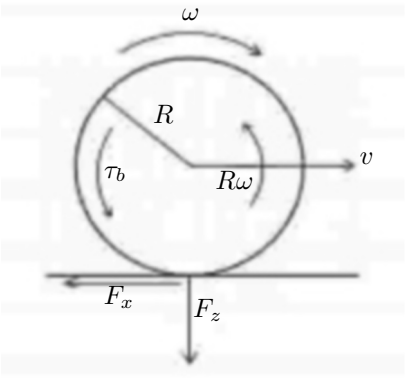

Fig. 1. Quarter-car braking model.

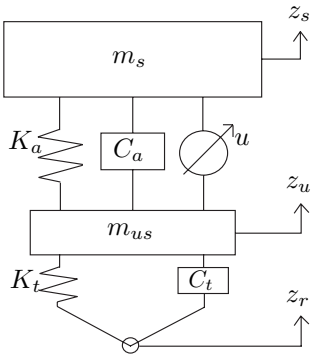

Fig. 2. Two-DOF quarter-car active suspension model.

The quarter-car active suspension model shown in Fig. 2 is represented as a two degree-of-freedom (DOF) system. It consists of a single sprung mass (car body) connected to a unsprung mass (wheel). The suspensions between the sprung mass and unsprung mass are modeled as linear viscous damper and spring elements, while the tire is modeled as linear spring and damping elements. The equations of motion for this quarter-car active suspension model can be written as follows:

$$\begin{aligned} m_s\ddot{z}_s &= -K_a(z_s - z_u) - C_a(\dot{z}_s - \dot{z}_u) + u \\ m_{us}\ddot{z}_u &= K_a(z_s - z_u) + C_a(\dot{z}_s - \dot{z}_u) - u \\ &\quad -K_t(z_u - z_r) - C_t(\dot{z}_u - \dot{z}_r)\,, \end{aligned} \tag{2}$$

where z_s and z_u are the displacements of car body and wheel, m_s and m_{us} are the masses of car body and wheel, K_a and K_t are the spring coefficients, C_a and C_t are the damping coefficients, z_r is the road disturbance, and u is the control force from

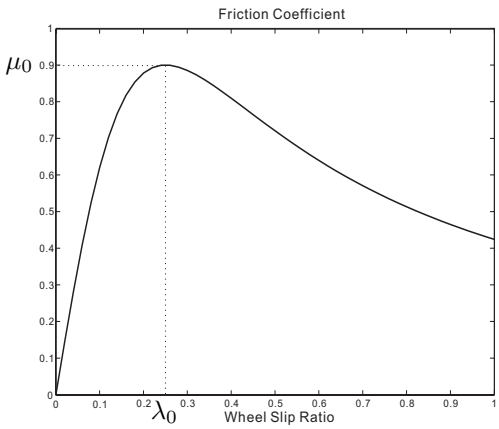

Fig. 3. The friction coefficient function $\mu(\lambda)$.

the hydraulic actuator. From (1) and (2), we can have

$$m = m_s + m_{us} \tag{3}$$

$$F_z = mg - K_t(z_u - z_r) - C_t\left(\dot{z}_u - \dot{z}_r\right), \tag{4}$$

where g is the acceleration of gravity.

In addition, the coefficient of friction $\mu(\lambda)$ is a nonlinear function of the wheel slip ratio λ. The wheel slip ratio λ is defined by

$$\lambda = \frac{v - R\omega}{v}, \tag{5}$$

and describes the normalized difference between the vehicle speed v and the speed of the wheel perimeter $R\omega$. The slip value of $\lambda = 0$ characterizes the free motion of the wheel where no friction force F_x is exerted. If the slip reaches the value $\lambda = 1$, then the wheel is locked ($\omega = 0$). The friction coefficient $\mu(\lambda)$ can span over a very wide range. The relationship between $\mu(\lambda)$ and wheel slip ratio λ is shown in Fig. 3. It shows how the friction coefficient $\mu(\lambda)$ increases with slip λ up to a value λ_0, where it attains its maximum value μ_0. For higher slip values, the friction coefficient will decrease until the wheel is locked. The function of $\mu(\lambda)$ can be approximated by the function

$$\mu\left(\lambda\right) = 2\mu_0 \frac{\lambda_0 \lambda}{\lambda_0^2 + \lambda^2} = \mu_0 f\left(\lambda\right)\lambda, \tag{6}$$

where μ_0 is maximum friction coefficient between tire and road, $f(\lambda) = 2\frac{\lambda_0}{\lambda_0^2+\lambda^2}$ is always positive, and λ_0 is the optimal slip ratio, which can yield the peak friction value $\mu(\lambda_0) = \mu_0$.

With the choices of the state variables $x_1 = v$, $x_2 = \omega$, $x_3 = \tau_b$, $x_4 = z_s$, $x_5 = \dot{z}_s$, $x_6 = z_u$, and $x_7 = \dot{z}_u$, the integrated braking system modeled by (1) and (2) can be rewritten as

$$\begin{aligned}
\dot{x}_1 &= -\frac{\mu(\lambda)F_z}{m} - \frac{C_x}{m}x_1^2 \\
\dot{x}_2 &= -\frac{B}{I}x_2 + \frac{\mu\left(\lambda\right)R}{I}F_z - \frac{1}{I}x_3 \\
\dot{x}_3 &= -\frac{1}{\tau}x_3 + \frac{K_b}{\tau}v_B \\
\dot{x}_4 &= x_5 \\
\dot{x}_5 &= -\frac{K_a}{m_s}(x_4 - x_6) - \frac{C_a}{m_s}(x_5 - x_7) + \frac{1}{m_s}u \\
\dot{x}_6 &= x_7 \\
\dot{x}_7 &= \frac{K_a}{m_{us}}(x_4 - x_6) + \frac{C_a}{m_{us}}(x_5 - x_7) - \frac{1}{m_{us}} \\
&\quad -\frac{K_t}{m_{us}}(x_6 - z_r) - \frac{C_t}{m_{us}}(x_7 - \dot{z}_r).
\end{aligned} \tag{7}$$

3. NONLINEAR BACKSTEPPING DESIGN

According to the system dynamics mentioned in the previous section, the control objective for the integrated anti-lock braking system is to keep the wheel slip ratio close to its optimal value and force the vehicle velocity to converge to zero as fast as possible. The goals are achieved by employing nonlinear backstepping schemes, whose design procedure consists of two parts to construct the anti-lock braking and active suspension controllers individually. First of all, the regulated variable for the braking design is introduced as

$$z_1 = v = x_1. \tag{8}$$

Then, the derivative of the regulated variable z_1 is computed as

$$\dot{z}_1 = \dot{x}_1 = -\frac{\mu(\lambda)}{m}F_z - \frac{C_x}{m}z_1^2. \tag{9}$$

From (5), the desired angular velocity is chosen as

$$\omega_d = \frac{1 - \lambda_0}{R}z_1, \tag{10}$$

which implies that the wheel slip ratio attains the value yielding the maximum friction coefficient. With the choice of the virtual control $x_2 = \omega$, the corresponding error state variable is defined as

$$z_2 = x_2 - \omega_d. \tag{11}$$

Therefore, the derivative of the error state variable z_2 is computed as follows:

$$\begin{aligned}
\dot{z}_2 &= \dot{\omega} - \dot{\omega}_d \\
&= -\frac{B}{I}x_2 + \frac{F_z R}{I}\mu\left(\lambda\right) - \frac{1}{I}x_3 \\
&\quad - \frac{1 - \lambda_0}{R}\left(-\frac{F_z}{m}\mu\left(\lambda\right) - \frac{C_x}{m}z_1^2\right).
\end{aligned} \tag{12}$$

Since x_3 is used as the virtual control variable, we choose the stabilizing function as

$$\begin{aligned}
\alpha_1 &= I\frac{\mu_0 f(\lambda)R}{m}[mg - K_t(x_6 - z_r) - C_t(x_7 - \dot{z}_r)] \\
&\quad - Bx_2 + I\frac{1 - \lambda_0}{R}\frac{\mu(\lambda)}{m}[mg - K_t(x_6 - z_r) \\
&\quad - C_t(x_7 - \dot{z}_r)] + F_z R\mu(\lambda) + I\frac{1 - \lambda_0}{R}\frac{C_x}{m}z_1^2 \\
&\quad + Ik_2 z_2,
\end{aligned} \tag{13}$$

where k_2 is a positive design constant. With the choice of the corresponding error state variable

$$z_3 = x_3 - \alpha_1 \,, \tag{14}$$

the derivative of z_3 is computed as

$$\begin{aligned}\dot{z}_3 &= \dot{x}_3 - \dot{\alpha}_1 \\ &= -\frac{1}{\tau}x_3 + \frac{K_b}{\tau}v_b - \left[I\frac{1}{m}\mu_0 R f_1 - B f_2 + R f_3 \right. \\ &\quad \left. + I\frac{1-\lambda_0}{R}\frac{1}{m}f_3 + I\frac{1-\lambda_0}{R}\frac{C_x}{m}f_4 + I k_2 f_5 \right],\end{aligned} \tag{15}$$

where

$$\begin{aligned}f_1 &= f(\lambda)[-K_t(x_7 - \dot{z}_r) - C_t f_6] - \frac{\lambda f^2(\lambda)}{\lambda_0} f_7 f_8 \\ f_2 &= \frac{R}{I}\mu(\lambda) f_8 - \frac{B}{I}x_2 - \frac{1}{I}(z_3 + \alpha_1) \\ f_3 &= f(\lambda)[-K_t(x_7 - \dot{z}_r) - C_t f_6] + \mu_0 f(\lambda) f_7 f_8 \\ f_4 &= -\frac{2z_1}{m}\left[\mu(\lambda) f_8 + C_x z_1^2\right] \\ f_5 &= -\frac{B}{I}x_2 + \frac{F_z R}{I}\mu(\lambda) - \frac{1}{I}(z_3 + \alpha_1) \\ &\quad + \frac{1-\lambda_0}{mR}\left[\mu(\lambda) f_8 + C_x z_1^2\right] \\ f_6 &= \frac{1}{m_{us}}\left[K_a(x_4 - x_6) + C_a(x_5 - x_7) - 1\right] \\ &\quad + \frac{1}{m_{us}}(f_8 - mg) - \ddot{z}_r \\ f_7 &= \frac{R}{I x_1}(B x_2 + x_3) - \mu_0 f_8 \frac{f(\lambda)\lambda}{x_1}\left(\frac{R^2}{I} + \frac{R x_2}{M x_1^2}\right) \\ f_8 &= mg - K_t(x_6 - z_r) - C_t(x_7 - \dot{z}_r)\,.\end{aligned}$$

Since the actual control input v_b appears in (15), we can choose our control law as

$$\begin{aligned}v_b = &\frac{\tau z_2}{K_b I} + \frac{1}{K_b}(z_3 + \alpha_1) + \frac{\tau}{K_b}\left(\frac{I}{m}\mu_0 R f_1 - B f_2 \right. \\ &\left. + R f_3 + \frac{1-\lambda_0}{mR}(I f_3 + C_x I f_4) + I k_2 f_5\right) \\ &- \frac{\tau}{K_b}k_3 z_3 \,,\end{aligned} \tag{16}$$

where k_3 is a positive design constant.

After the further investigation, a key point has been found out that the normal force can be adapted by following the change of x_6. It implies that the normal force can be adjusted to help the braking performance if x_6 is close to a desired reference x_{6d}, which is represented by

$$x_{6d} = h(t)\,, \tag{17}$$

where $h(t)$ is the desired design function to be chosen later. Then a new regulated variable z_6 is selected in the following to stabilize the active suspension system:

$$z_6 = x_6 - h(t) - \kappa(x_4 + \frac{m_s}{m_{us}}x_5 + x_7)\,, \tag{18}$$

where κ is a design constant to be chosen. Then, we compute the derivative of z_6 as

$$\dot{z}_6 = x_7 - \dot{h} - \kappa(x_5 + \frac{m_s}{m_{us}}\dot{x}_5 + \dot{x}_7)\,. \tag{19}$$

The state x_7 is chosen as the virtual control variable, and the corresponding error state variable is defined as

$$z_7 = x_7 - \alpha_2\,, \tag{20}$$

for which we choose the stabilizing function

$$\begin{aligned}\alpha_2 = \frac{1}{A_1}&\left[\dot{h} - \kappa\frac{K_t}{m_{us}}h - A_2 x_5 - \kappa^2\frac{K_t}{m_{us}}x_4 \right. \\ &\left. - \kappa\frac{K_t}{m_{us}}(z_6 - z_r) + \kappa\frac{C_t}{m_{us}}\dot{z}_r - k_6 z_6\right],\end{aligned} \tag{21}$$

where

$$\begin{aligned}A_1 &= 1 + \kappa^2\frac{K_t}{m_{us}} + \kappa\frac{C_t}{m_{us}} \\ A_2 &= -\kappa + \kappa^2\frac{K_t m_s}{m_{us}^2}\,,\end{aligned}$$

and k_6 is a positive design constant. Therefore, (19) can be rewritten as follows:

$$\dot{z}_6 = A_1 z_7 - k_6 z_6\,. \tag{22}$$

The derivative of the error state z_7 is computed as follows:

$$\begin{aligned}\dot{z}_7 = &\left(\frac{A_2}{A_1 m_s} - \frac{1}{m_{us}}\right)u - \frac{K_t}{m_{us}}(x_6 - z_r) - \frac{1}{A_1}\ddot{h} \\ &+ \left(\frac{K_a}{m_{us}} - \frac{A_2 K_a}{A_1 m_s}\right)(x_4 - x_6) - \frac{\kappa C_t}{A_1 m_{us}}\ddot{z}_r \\ &+ \left(\frac{C_a}{m_{us}} - \frac{A_2 C_1}{A_1 m_s}\right)(x_5 - x_7) + \frac{\kappa^2 K_t}{A_1 m_{us}}x_5 \\ &- \frac{C_t}{m_{us}}(x_7 - \dot{z}_r) + \frac{\kappa K_t}{A_1 m_{us}}(\dot{h} - \dot{z}_r) \\ &+ \left(\frac{k_6}{A_1} + \frac{\kappa K_t}{A_1 m_{us}}\right)(A_1 z_7 - k_6 z_6)\,.\end{aligned} \tag{23}$$

Since the actual active suspension control input u appears in (23), we can design the controller as

$$\begin{aligned}u = &K_a(x_4 - x_6) + C_a(x_5 - x_7) - \frac{A_1}{A_3}z_6 \\ &+ \frac{1}{A_3}\left[\frac{K_t}{m_{us}}(x_6 - z_r) + \frac{C_t}{m_{us}}(x_7 - \dot{z}_r) \right. \\ &+ \frac{\ddot{h}}{A_1} - \frac{\kappa K_t}{A_1 m_{us}}\dot{h} - \frac{\kappa^2 K_t}{A_1 m_{us}}x_5 - k_7 z_7 \\ &\left. - \left(\frac{k_6}{A_1} + \frac{\kappa K_t}{A_1 m_{us}}\right)(A_1 z_7 - k_6 z_6)\right],\end{aligned} \tag{24}$$

where

$$\begin{aligned}A_3 &= -\frac{1}{m_{us}} + \frac{A_2}{A_1 m_s} \\ A_4 &= \frac{\kappa K_t + C_t}{A_3 m_{us} m_s}\,.\end{aligned}$$

Since there are five steps in our backstepping design procedure, the zero dynamics of the system is observed as follows:

$$\begin{aligned} \dot{x}_4 &= x_5 \\ \dot{x}_5 &= b_1 x_4 + b_2 x_5 + d\,, \end{aligned} \tag{25}$$

where

$$\begin{aligned} b_1 &= \frac{\kappa K_t}{A_3 m_{us} m_s} - \kappa^2 \frac{A_4 K_t}{A_1 m_{us}} \\ b_2 &= \frac{\kappa K_t}{A_3 m_{us}^2} - \frac{\kappa^2 K_t}{A_1 A_3 m_{us} m_s} - \frac{A_2 A_4}{A_1} \\ d &= \left(\frac{K_t}{A_3 m_{us} m_s} - \kappa \frac{A_4 K_t}{A_1 m_{us}}\right) h \\ &\quad + \left(\frac{A_4}{A_1} - \frac{\kappa K_t}{A_1 A_3 m_{us} m_s}\right) \dot{h} + \frac{\ddot{h}}{A_1 A_3 m_s}\,. \end{aligned}$$

The forms of b_1 and b_2 look like variables, but they are constants if an appropriate design constant κ is chosen. Since d is a bounded signal from the desired reference, if an appropriate value of κ is selected to ensure b_1 and b_2 to be negative, then the zero dynamics in (25) becomes stable.

After finishing the backstepping control design procedure, the Lyapunov function candidate is selected in the following for the analysis of system stability:

$$V = \frac{1}{2} z_1^2 + \frac{1}{2} z_2^2 + \frac{1}{2} z_3^2 + \frac{1}{2} z_6^2 + \frac{1}{2} z_7^2\,. \tag{26}$$

From (9), (12)-(16) and (22)-(24), the derivative of (26) is computed as follows:

$$\begin{aligned} \dot{V} &= z_1 \dot{z}_1 + z_2 \dot{z}_2 + z_3 \dot{z}_3 + z_6 \dot{z}_6 + z_7 \dot{z}_7 \\ &= z_1 \left(-\frac{F_z}{m} \mu(\lambda) - \frac{C_x}{m} z_1^2 \right) \\ &\quad + z_2 \left[-\frac{B}{I} x_2 + \frac{F_z R}{I} \mu(\lambda) - \frac{1}{I}(z_3 + \alpha_1) \right. \\ &\quad \left. - \frac{1-\lambda_0}{R} \left(-\frac{F_z}{m} \mu(\lambda) - \frac{C_x}{m} z_1^2 \right) \right] \\ &\quad + z_3 \left[-\frac{1}{\tau} x_3 + \frac{K_b}{\tau} v_b - \frac{I}{m} \mu_0 R f_1 + B f_2 \right. \\ &\quad \left. - R f_3 - \frac{1-\lambda_0}{mR} I (f_3 + C_x f_4) - I k_2 f_5 \right] \\ &\quad + z_6 (A_1 z_7 - k_6 z_6) \\ &\quad + z_7 \left[\left(-\frac{1}{m_{us}} + \frac{A_2}{A_1 m_s} \right) u - \frac{K_t}{m_{us}} (x_6 - z_r) \right. \\ &\quad + \left(\frac{K_a}{m_{us}} - \frac{A_2 K_a}{A_1 m_s} \right) (x_4 - x_6) - \frac{\kappa C_t}{A_1 m_{us}} \ddot{z}_r \\ &\quad + \left(\frac{C_a}{m_{us}} - \frac{A_2\, C_1}{A_1\, m_s} \right) (x_5 - x_7) + \frac{\kappa^2 K_t}{A_1 m_{us}} x_5 \\ &\quad - \frac{C_t}{m_{us}} (x_7 - \dot{z}_r) + \frac{\kappa K_t}{A_1 m_{us}} (\dot{h} - \dot{z}_r) \\ &\quad \left. + \left(\frac{k_6}{A_1} + \frac{\kappa K_t}{A_1 m_{us}} \right) (A_1 z_7 - k_6 z_6) - \frac{1}{A_1} \ddot{h} \right] \\ &= -\left(\frac{C_x}{m} z_1^2 + \frac{F_z}{m} \mu_0 f(\lambda) \lambda_0 \right) z_1 \\ &\quad - k_2 z_2^2 - k_3 z_3^2 - k_6 z_6^2 - k_7 z_7^2\,. \end{aligned} \tag{27}$$

Table 1. System parameter values of the integrated anti-lock braking system.

Parameter	Value	Parameter	Value
m	390 kg	K_b	0.8
m_s	350 kg	μ_0	0.9
m_{us}	40 kg	λ_0	0.25
R	0.25 m	τ	0.01 s
B	0.08 kgm^2	C_x	0.856 kg/m
K_a	19960 N/m	C_a	1050 Ns/m
K_t	175500 N/m	C_t	1500 Ns/m

Table 2. Design constants used in the integrated anti-lock braking system.

Parameter	Value	Parameter	Value
k_2	100	k_3	100
k_6	100	k_7	100
κ	0.0001		

Since $f(\lambda)$ is always positive, λ_0 is the optimal slip ratio with $0 < \lambda_0 \leq 1$, μ_0 is the corresponding peak friction value with $\mu_0 > 0$, and z_1 is the vehicle velocity which is always positive during braking process, we can conclude that $\dot{V}$ is negative definite with the appropriate choices of k_2, k_3, k_6, k_7 and κ. This result shows that the error system (z_1, z_2, z_3, z_6, z_7) is asymptotically stable according to Lyapunov stability theorem. In addition, the backstepping control design is also to stabilize the zero dynamic system (x_4, x_5) simultaneously. As a result, the controllers of the anti-lock braking and active suspension systems can keep the wheel slip ratio λ close to its optimal value λ_0, and then force the vehicle speed to converge to zero at a shorter braking distance.

4. SIMULATION RESULTS

The system parameters of the anti-lock braking model combined with active suspensions are given in Table 1, and all the design constants are chosen in Table 2. The road surface is corresponding to dry asphalt. The maximum control torque from the anti-lock braking system is assumed to be 1500 Nm. The desired design function $h(t)$ in (17) is simply assumed to be a constant, which is selected to be -0.005. In addition, the initial velocity of the vehicle is 30 m/s and the corresponding initial wheel angular velocity is 123.67 rad/s resulting in $\dot{v}(0) = 0$.

Fig. 4 shows that the vehicle speed and wheel speed during braking process with three different braking control schemes. The diamond line denotes the vehicle speed and the star line is the wheel angular speed. The dotted-dashed line shows that the system employs the maximum constant braking torque and its wheel speed fast reaches zero at 0.3 s, but its vehicle velocity stops to zero around 6.3 s. It implies that the wheel is completely locked at 0.3 s and the system must

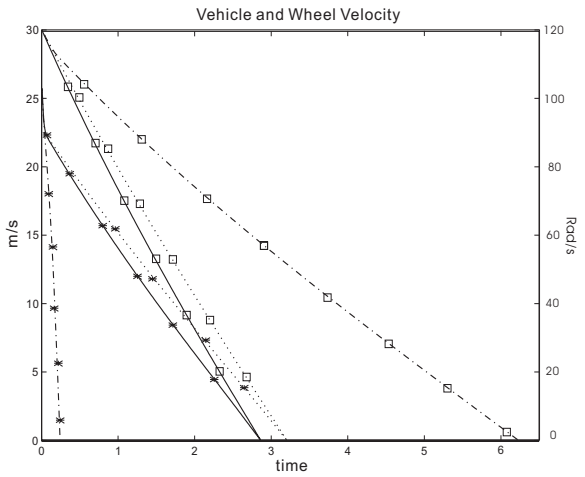

Fig. 4. The vehicle and wheel speeds with the use of different braking schemes.

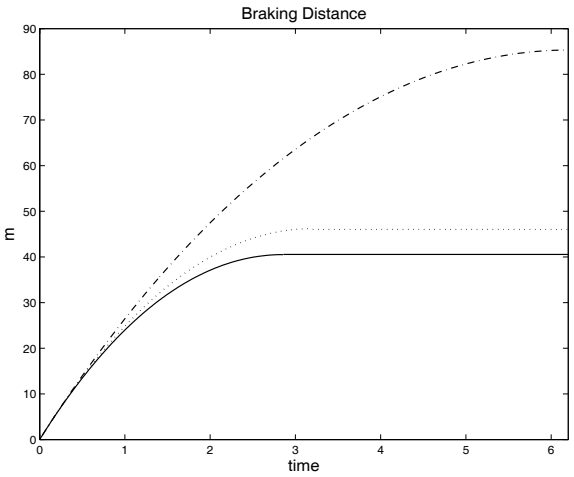

Fig. 5. The required braking distances with the use of different braking schemes.

spend almost $6.3\,s$ to stop the vehicle. The solid line illustrates that the integrated plant combining anti-lock braking system with active suspension system can stop the car at $2.9\,s$ and has the most excellent performance compared to the dotted-dashed line and dotted line, which represents the system using ABS only without the assistance of active suspensions.

The braking distances with three different braking designs are shown in Fig. 5. The dashed-dotted line shows that the system with the maximum braking torque has to spend almost $86\,m$ to stop the vehicle. The dotted line shows that the system using only ABS must spend $47\,m$ to stop the car. Obviously, the solid line illustrates that the integrated braking system combined with active suspensions has the most excellent performance and can stop the car around $43\,m$.

5. CONCLUDING REMARKS

In this paper, a nonlinear backstepping control design scheme has been developed for the control of a quarter-car anti-lock braking system combined with active suspensions. In addition, an algorithm for integrating these two subsystems is proposed, and two individual controllers have been designed and coordinated with this integrated algorithm. As a result, the integrated anti-lock braking system with the assistance of active suspensions can obtain excellent braking performance because of reduction of braking time and distance.

In the further research, adaptive backstepping control strategy should be considered and employed for the design of anti-lock braking systems with dynamic uncertainties. In addition, a half-car (even a full-car) system model would be another interesting issue, since it would make the system become more realizable. Hence, how to design a more robust controller for further enhancing the performance of anti-lock braking systems is a new challenge to be faced on in future works.

REFERENCES

Alleyne, A. (1997). Improved vehicle performance using combined suspension and braking forces. *Vehicle System Dynamics* **27**, 235–265.

Alvarez, L., J. Yi, X. Claeys and R. Horowitz (2003). Emergency braking control with an observer-based dynamic tire/toad friction model and wheel angular velocity measurement. *Vehicle System Dynamics* **39**, 81–97.

Drakunov, S.V., B. Ashrafi and A. Rosiglioni (2000). Yaw control algorithm via sliding mode control. Vol. 1. pp. 580–583. Chicago, Illinois.

Drakunov, S.V., U. Ozguner, P. Dix and B. Ashrafi (1995). ABS control using optimum search via sliding modes. *IEEE Transactions on Control Systems Technology* **3**, 79–85.

Khalil, H.K. (2002). *Nonlinear Systems, 3rd ed.*. Upper Saddle River, NJ: Prentice-Hall.

Kim, E.-S (1996). Nonlinear indirect adaptive control of a quarter car active suspension. pp. 61–66. Dearborn, MI.

Krstić, M., I. Kanellakopoulos and P. V. Kokotović (1995). *Nonlinear and Adaptive Control Design*. New York, NY: John Wiley & Sons.

Lin, J.-S. and I. Kanellakopoulos (1997). Nonlinear design of active suspensions. *IEEE Control Systems Magazine* **17**, 45–59.

Liu, Y. and J. Sun (1995). Target slip tracking using gain-scheduling for antilock braking systems. Vol. 2. pp. 1178–1182. Seattle, Washington.

Unsal, C. and P. Kachroo (1999). Sliding mode measurement feedback control for antilock braking systems. *IEEE Transactions on Control Systems Technology* **7**, 271–281.